

Styrene-Butadiene-Styrene Block Copolymer 위 이온빔 조사를 이용한 주름 구조 생성 메커니즘 연구

이주환¹, 김대현² 

¹ 연세대학교 전기전자공학부

² 한국폴리텍대학 스마트전기학과

Mechanism of Wrinkle Formation on Styrene-Butadiene-Styrene Block Copolymer via Ion-Beam Irradiation

Ju Hwan Lee¹ and Dai-Hyun Kim²

¹ Department of Electrical and Electronic Engineering, Yonsei University, Seoul 03722, Korea

² Department of Smart Electric, Korea Polytechnic, Incheon 22121, Korea

(Received January 18, 2021; Revised February 1, 2021; Accepted February 2, 2021)

Abstract: Wrinkle patterns were fabricated on styrene-butadiene-styrene (SBS) block copolymer substrates using ion-beam (IB) irradiation with various intensities. The wavelength of the wrinkle pattern increased as the IB intensity was increased from 800 to 1,600 eV. IB irradiation-induced changes in the surface properties that were confirmed via physicochemical surface analyses. X-ray photoelectron spectroscopy analysis revealed chemical surface reformation due to the IB irradiation, resulting in C-O/C=O bonds after IB irradiation that were not reported before. These results indicate that the surface chemical modification caused by IB irradiation is strongly related to the surface modulus, which is important when fabricating wrinkle patterns. Furthermore, a strong IB irradiation induced a strong compressive strain; thus the size of the wrinkle pattern was increased.

Keywords: Ion-beam irradiation, Wrinkle formation, Styrene-butadiene-styrene block copolymer

1. INTRODUCTION

Wrinkle patterns are commonly observed in daily life and many researchers have tried to apply them in science and technology [1,2]. Various materials have been used to fabricate the wrinkle pattern, such as soft materials with elastomers [3]. Thermoplastic elastomers are copolymers which have good thermoplastic and elastomeric properties,

so they are flexible with a low modulus value like rubbery materials [4]. Thermoplastic elastomers can be classified into block copolymers and thermoplastic/elastomer blends. Styrene-butadiene-styrene (SBS), a thermoplastic elastomer, is a strong good candidate for fabricating wrinkle patterns as it behaves like rubber at room temperature and has good mechanical properties and glassy/rubbery domains [5]. Because of its favorable properties, it is used in various industries, such as adhesives manufacture, footwear, and asphalt [6].

The reason for using elastomeric materials in wrinkle formation processes is to achieve a modulus difference in adjoining layers induced by compressive stress that leads

✉ Dai-Hyun Kim; kdh978@naver.com

Copyright ©2021 KIEEME. All rights reserved.
This is an Open-Access article distributed under the terms of the Creative Commons Attribution Non-Commercial License (<http://creativecommons.org/licenses/by-nc/3.0>) which permits unrestricted non-commercial use, distribution, and reproduction in any medium, provided the original work is properly cited.

to a wrinkle pattern that occurs between the elastomeric bulk and the top (stiff) layer [7]. The latter can be generated by various methods, such as plasma treatment with various gases [8], metal deposition [9], with thermal curable resins [10], and ion-beam (IB) irradiation. After compressive stress has been applied, the status of the top (stiff) layer determines the results such as wrinkling, folding, or delamination. The fabricated wrinkle pattern can improve the optical [11], mechanical [12] and electrical properties [13], and so it can be used in a wide range of applications, such as stretchable devices [14], and lithography free patterning [15].

Herein, we demonstrate the fabrication of a wrinkle pattern on SBS surfaces using IB irradiation at several energy intensities. To confirm the creation of the wrinkle pattern, we conducted field-emission scanning electron microscopy (FE-SEM), with the entire surface being observed as a function of IB irradiation energy. IB irradiation can induce not only physical but also chemical surface modification, and so X-ray photoelectron spectroscopy (XPS) was used to examine the changes in the surface chemical composition of SBS caused by the IB irradiation. Atomic force microscopy (AFM) was conducted to obtain specific surface information; the values of the wavelength and amplitude of the wrinkle patterns were collected via a line profile program applied to the AFM images.

2. METHOD FOR EXPERIMENT

2.1 SBS thin-film fabrication on glass substrates

10 wt% SBS powder (styrene 21%) was dissolved in toluene, after which the solution was stirred with 420 rpm for 2 h at 75°C followed by aging for at least 1 day. The prepared SBS solution was spin-coated onto glass substrates (dimensions: 32×22×11 mm³) at 3,000 rpm for 30s. Before spin-coating, the glass substrates were cleaned using acetone, methanol, and deionized water for 10 min each and then dried with N₂ gas. After the spin-coating process, samples were annealed at 65°C for 2 h to remove any residual solvent.

2.2 IB treatment on the SBS sample for wrinkle formation

After the annealing process, SBS samples were placed in a vacuum chamber to be irradiated by IB with an advanced DuoPIGatron-type IB system; the pressure was set at 5×10⁻⁵ Torr with 1 sccm of Ar gas flow ing into the vacuum chamber. The SBS samples were irradiated for 1 min with an IB intensity of either 800 or 1,600 eV. The IB exposure conditions used a positively charged current density of 1.0 mA/cm².

2.3 Investigation of the wrinkle pattern on the SBS surface

FE-SEM (Quanta 200 FEG; FEI Company, Singapore) was conducted to verify the morphology change of the SBS samples surface due to IB irradiation. Specific information for the wrinkle pattern on the SBS surface was obtained by using AFM (XE-200; Park Systems, South Korea). Furthermore, depth and wavelength information of the wrinkle patterns were collected by using line profile analysis (XEI software, Park Systems).

2.4 Verification of surface characteristics related to IB irradiation exposure

Chemical composition change of the SBS surface was observed as the IB intensity was increased using XPS (K-alpha, Thermo VG, U.K). XPS spectra of carbon and oxygen were investigated before and after IB irradiation.

3. RESULTS AND DISCUSSIONS

Figure 1(a)~(c) shows FE-SEM images of the morphology on the SBS surface as a function of IB intensity. From these images, we confirmed that unlike the non-IB-irradiated sample, IB intensities of 800 and 1,600 eV created clear wrinkle patterns on the SBS surfaces. This indicates that the IB irradiation strongly affected the formation of the wrinkled structure on the SBS surface. Furthermore, when comparing the IB intensities of 800 and 1,600 eV, we also confirmed that the size of the

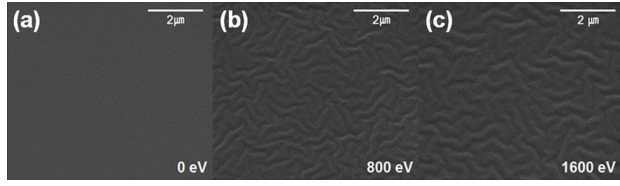


Fig. 1. FE-SEM surface morphological images of the SBS surface: (a) 0 eV, (b) 800 eV, and (c) 1,600 eV.

wrinkle pattern increased as the IB energy intensity increased. Typically, it is known that IB irradiation is a useful method to change the chemical composition of a polymer surface, leading to modification of the mechanical properties of the irradiated surface. To fabricate the wrinkled structure on an elastic substrate, a stiff top skin layer is required to produce a modulus mismatch between the substrate and the surface [7]. In our case, the mechanical properties of irradiated SBS surface were changed and a stiff skin layer was formed due to chemical composition modification by the IB irradiation. Furthermore, during this process, the irradiated surface of the SBS swelled and contracted at nearly the same time due to ion penetration by the IB, and this phenomenon acted as an external force to generate strain. Consequently, the effect of IB irradiation on the SBS surface induced a wrinkled structure.

XPS analysis was conducted to verify the chemical modification due to the IB irradiation of the SBS surface. C 1s XPS spectra of the SBS surface at IB intensities of 0, 800, and 1,600 eV are presented in Fig. 2(a)–(c). IB intensity of 0 eV (no irradiation) had one peak located at 284.8 eV which indicates carbon single bonds (C-C) and double bonds (C=C) in the SBS chemical structure. Because SBS consists of styrene and butadiene blocks, only carbon bonds were observed at an IB intensity of 0 eV. However, significant phenomena were observed in the XPS spectra after IB irradiation of the SBS surface. First, after IB irradiation, the C 1s peak consisted of three sub-peaks located at 284.7, 268.3, and 288.0 eV, inferring the presence of C-C/C=C bond (at an IB intensity of 0 eV only), carbon-oxygen single bonds (C-O), and carbon-oxygen double bonds (C=O), respectively. These sub-peaks indicate that IB irradiation on the SBS surface broke the C-C/C=C bonds and induced the generation of

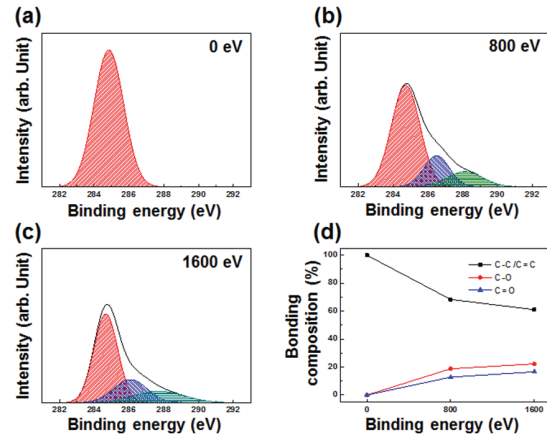


Fig. 2. XPS C 1s core-level spectra of SBS after exposure to IB intensities of (a) 0 eV, (b) 800 eV, and (c) 1,600 eV. (d) Bonding composition percentage graph as a function of IB intensity. The graph shows changes in the number of carbon bonds with increased IB intensity.

C-O and C=O bonds. The second significant phenomenon is the change in XPS spectra composition percentage as the IB intensity increased: the percentage of C-C/C=C bonds decreased while that of C-O/C=O bonds increased [Fig. 2(d)].

To sum up, the results from the XPS spectra indicate that IB irradiation broke the C-C/C=C bonds which were then reconstructed with nearby oxygen atoms to produce a more stable structure. During this process, the broken polymer chains were cross-linked due to oxygen atoms forming C-O/C=O bonds and the skin layer was induced which had a higher modulus value than the SBS substrate. In the bucking theory, the wavelength of the wrinkle pattern is expressed as

$$\lambda = 2\pi h \left(\frac{E_f}{3E_s} \right)^{\frac{1}{3}} \quad (1)$$

where h , E_f , and E_s are the thickness of the top (stiff) layer and the plane strain modulus value of the top (stiff) layer and substrate, respectively. Accordingly, modulus mismatch between the surface and substrate must be achieved to fabricate the wrinkled structure on the SBS surface, a condition that was met due to the IB irradiation. Hence, a wrinkled structure was fabricated

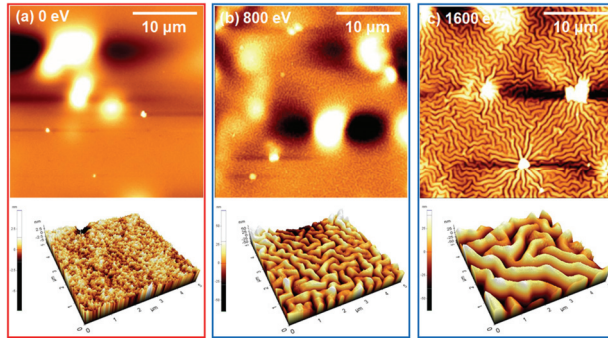


Fig. 3. AFM ($30 \times 30 \mu\text{m}$) with 3D topological images ($5 \times 5 \mu\text{m}$) of the SBS wrinkle pattern after exposure to IB irradiation energy levels of (a) 0 eV, (b) 800 eV, and (c) 1,600 eV.

on the SBS surface. Furthermore, because of this, C-O/C=O bonds can be observed in the XPS spectra after IB irradiation. Additionally, it can be observed that as the IB energy intensity increased, the number of C-O/C=O bonds increased, thus a higher surface modulus value was caused by the higher IB irradiation energy. Hence, the IB irradiation induced surface chemical modification and increased the surface modulus value by generating C-O/C=O bonds that strongly affected the fabrication of the wrinkle pattern on the SBS surface.

Specific information on the SBS surface as a function of IB intensity was investigated using AFM. Figure 3 (a)–(c) shows AFM surface images with 3-D topological images of the SBS wrinkle pattern at IB intensities of 0, 800, and 1,600 eV, respectively. No significant surface topology was observed before IB irradiation, while after IB irradiation at 800 and 1,600 eV, wrinkled structures can be observed in the AFM images, a result which fits with the results of the FE-SEM analysis. Furthermore, a random labyrinth pattern was observed on the SBS surface, from which the direction of compressive strain induced by IB irradiation can be estimated [16]. The morphology of the wrinkle pattern is determined by the direction of compressive strain. Commonly, isotropic and anisotropic compressive strain induces a random wrinkle pattern and a biased pattern, respectively. Therefore, in this case, it is obvious that the IB irradiation induced isotropic forces on the SBS surface evenly and a random labyrinth wrinkle pattern was achieved regardless of irradiation energy. Additionally, it was clearly verified through the 3D

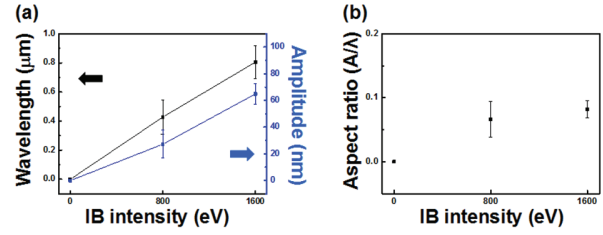


Fig. 4. (a) Wavelength and amplitude of the wrinkled structure on an IB-irradiated SBS surface as a function of irradiation energy (indicated by the black and blue graphs, respectively) and (b) a calculated aspect ratio (amplitude/wavelength; A/λ) graph of the wrinkled structure on the SBS surface.

topology images that the size of the wrinkled structure in term of wavelength and amplitude was increased by the increase in IB energy intensity. The higher the IB energy intensity, the greater the size of the wrinkled structure.

By applying line profiling to the AFM images, we investigated the exact numerical values of the wavelength and amplitude of the wrinkle pattern on the SBS. The values were collected more than 15 times typical wrinkle patterns. Figure 4(a) shows the graph of the wavelength (black line) and amplitude (blue line) of the wrinkle pattern on the SBS as a function of IB intensity. The IB intensity of 800 eV produced a wrinkle pattern with a wavelength of $0.428 \mu\text{m}$ and an amplitude of 27.202 nm, while the IB intensity of 1,600 eV resulted in a wrinkle pattern with a wavelength of $0.805 \mu\text{m}$ and the amplitude of 64.869 nm. Furthermore, numerical values of the wrinkle pattern on the SBS show the significant change as an IB intensity increased. As presented in equation (1), the wavelength is affected by modulus difference and the thickness of top layer. Additionally, the amplitude can be described as

$$A = h \sqrt{\frac{\varepsilon - \varepsilon_c}{\varepsilon_c}} \quad (2)$$

where ε is the compressive strain and ε_c is threshold critical strain which can be estimated as $\varepsilon_c \approx 0.25 (3Es/E_t)^{2/3}$. The amplitude is also affected by the thickness of the top layer and furthermore, the compressive strain is the main factor to determine the amplitude of the wrinkle pattern [7]. This indicates that the higher intensity of IB

irradiation on the SBS surface affected these conditions strongly. Figure 4(b) presented aspect ratio (the ratio of the wavelength to amplitude) of the wrinkle pattern on the SBS as a function of IB intensity. The aspect ratio of the wrinkle pattern on the SBS at an IB intensity of 800 and 1,600 eV was 0.06632 and 0.08178, respectively. As there is a strong mathematical relationship between the aspect ratio and surface modulus, it is possible to estimate the tendency of the surface modulus to change with increasing IB intensity through the aspect ratio. As the IB intensity increased, the aspect ratio increased, which indicates that the surface modulus increased as the IB intensity increased.

Wrinkle formation and the change in pattern size were investigated through the aforementioned analyses, and the mechanism of wrinkled structure formation was identified by putting the results of these together, as shown in Fig. 5. Chemical modification of the irradiated surface occurred and the surface modulus value was modified by the IB irradiation, and due to this, modulus mismatch between the surface and substrate (the minimal condition for wrinkle fabrication) was induced. Furthermore, ion collisions on the IB-irradiated surface induced swelling and contraction which incurred compressive strain that led to achieving the wrinkled structure on the SBS surface [Fig. 5(a)]. There was a significant difference in the wrinkle pattern sizes when comparing IB energy intensities of 800 and 1,600 eV [Fig. 5(b) and (c)]. As the IB energy increased, the ion penetration depth increased, and this is directly related to the thickness of the top (stiff) layer. Therefore, at the higher IB energy, a thicker stiff layer (h_2) was achieved. Furthermore, the higher IB irradiation energy induced more ion collisions with stronger swelling and contraction of the surface. Because of this, the compressive strain became stronger at 1,600 eV (ϵ_2) than 800 eV (ϵ_1). As investigated previously, the amplitude and wavelength of the wrinkle pattern were determined by the thickness of the top (stiff) layer and the applied compressive strain. Thus, the wrinkle pattern size became bigger with IB energy of 1,600 eV (A_2) than 800 eV (A_1). Consequently, the amplitude and wavelength of the wrinkled structure on the SBS surface can be controlled by changing the IB irradiation energy.

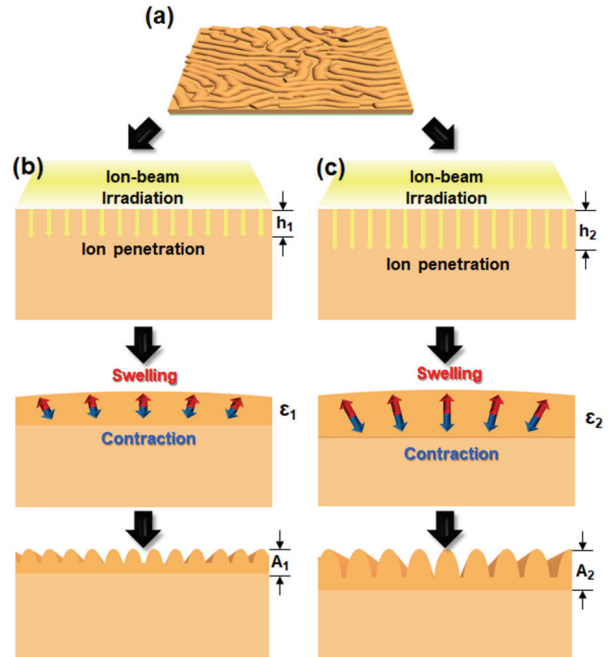


Fig. 5. Schematic of wrinkle formation on the SBS surface as the IB irradiation energy increased: (a) the fabricated wrinkled structure on the SBS surface and the mechanism of wrinkle formation at (b) low, and (c) high IB energy intensity. h , ϵ , and A indicate the depth of the stiff layer, the compressive strain, and the amplitude of the wrinkled structure, respectively.

4. CONCLUSION

We investigated the fabrication of wrinkled structures on SBS surfaces induced by IB irradiation. Significant surface modification was observed on the SBS surface after IB irradiation regardless of the IB irradiation energy. This indicates that the conditions for producing wrinkled structures were satisfied by the IB irradiation. Modification of the chemical composition of the surface was observed via XPS. C-C/C=C bonds were broken and recombined with nearby oxygen atoms due to the IB irradiation to produce a stable structure. During this process, polymer chains were cross-linked and the IB-irradiated surface became harder than before, which induced the modulus mismatch between the surface and the substrate necessary for wrinkle formation. Specific information on the surface morphology was obtained by conducting an AFM analysis. As the IB irradiation energy increased, the wrinkle pattern size in term of

amplitude and wavelength increased. Furthermore, changes in the surface modulus value measured using the aspect ratio as the IB energy increased could be estimated. It was confirmed that the size of the wrinkle pattern can be determined by the level of IB irradiation energy. At higher IB irradiation energy, the ions penetrated deeper, which induced a thicker stiff layer. In addition, strong compressive strain was created at the higher IB energy, resulting in a larger sized wrinkled structure. To sum up, the controllability of the wrinkle pattern size can be achieved by changing the IB irradiation energy level.

ORCID

Dai-Hyun Kim

<https://orcid.org/0000-0002-5441-3834>

REFERENCES

- [1] D. Yan, K. Zhang, F. Peng, and G. Hu, *Appl. Phys. Lett.*, **105**, 071905 (2014). [DOI: <https://doi.org/10.1063/1.4893596>]
- [2] P. Jurík, P. Slepíčka, M. Nagvová, and V. Švorčík, *Surf. Coat. Technol.*, **311**, 344 (2017). [DOI: <https://doi.org/10.1016/j.surfcoat.2017.01.030>]
- [3] T. Seki, D. Yamaoka, T. Takeshima, Y. Nagashima, M. Hara, and S. Nagano, *Mol. Cryst. Liq. Cryst.*, **644**, 52 (2017). [DOI: <https://doi.org/10.1080/15421406.2016.1277329>]
- [4] R. J. Spontak and N. P. Patel, *Curr. Opin. Colloid Interface Sci.*, **5**, 333 (2000). [DOI: [https://doi.org/10.1016/S1359-0294\(00\)00070-4](https://doi.org/10.1016/S1359-0294(00)00070-4)]
- [5] W. F. Lee and Y. J. Chen, *J. Appl. Polym. Sci.*, **82**, 2641 (2001). [DOI: <https://doi.org/10.1002/app.2117>]
- [6] M. D. Romero-Sánchez, M. M. Pastor-Blas, J. M. Martín-Martínez, and M. J. Walzak, *Int. J. Adhes. Adhes.*, **25**, 358 (2005). [DOI: <https://doi.org/10.1016/j.ijadhadh.2004.12.001>]
- [7] J. Y. Chung, A. J. Nolte, and C. M. Staffo, *Adv. Mater.*, **23**, 349 (2011). [DOI: <https://doi.org/10.1002/adma.201001759>]
- [8] X. Cheng, B. Meng, X. Chen, M. Han, H. Chen, Z. Su, M. Shi, and H. Zhang, *Small*, **12**, 229 (2016). [DOI: <https://doi.org/10.1002/sml.201502720>]
- [9] N. Bowden, S. Brittain, A. G. Evans, J. W. Hutchinson, and G. M. Whitesides, *Nature*, **393**, 146 (1998). [DOI: <https://doi.org/10.1038/30193>]
- [10] H. Hou, J. Yin, and X. Jiang, *Adv. Mater.*, **28**, 9126 (2016). [DOI: <https://doi.org/10.1002/adma.201602105>]
- [11] T. Ohzono, H. Monobe, R. Yamaguchi, Y. Shimizu, and H. Yokoyama, *Appl. Phys. Lett.*, **95**, 014101 (2009). [DOI: <https://doi.org/10.1063/1.3167547>]
- [12] B. Li, Y. P. Cao, X. Q. Feng, and H. Gao, *Soft Matter*, **8**, 5728 (2012). [DOI: <https://doi.org/10.1039/C2SM00011C>]
- [13] B. Wang, Y. Zhang, H. Zhang, Z. Chen, X. Xie, Y. Sui, X. Li, G. Yu, L. Hu, Z. Jin, and X. Liu, *Carbon*, **70**, 75 (2014). [DOI: <https://doi.org/10.1016/j.carbon.2013.12.074>]
- [14] M. Ramuz, B.C.K. Tee, J.B.H. Tok, and Z. Bao, *Adv. Mater.*, **24**, 3223 (2012). [DOI: <https://doi.org/10.1002/adma.201200523>]
- [15] C. Lu, H. Möhwald, and A. Fery, *Soft Matter*, **3**, 1530 (2007). [DOI: <https://doi.org/10.1039/B712706E>]
- [16] P. C. Lin and S. Yang, *Appl. Phys. Lett.*, **90**, 241903 (2007). [DOI: <https://doi.org/10.1063/1.2743939>]